Viscoelastic response of neural cells governed by the deposition of amyloid-β peptides (Aβ)

Ze Gong,[1,2,a)] Ran You,[3,a)] Raymond Chuen-Chung Chang,[3,4] and Yuan Lin[1,2,b)]
[1]*Department of Mechanical Engineering, University of Hong Kong, Hong Kong, China*
[2]*HKU-Shenzhen Institute of Research and Innovation (HKU-SIRI), Shenzhen, Guangdong, China*
[3]*Laboratory of Neurodegenerative Diseases, School of Biomedical Sciences, LKS Faculty of Medicine, The University of Hong Kong, Hong Kong, China*
[4]*State Key Laboratory of Brain and Cognitive Sciences, Hong Kong, China*

(Received 1 February 2016; accepted 14 May 2016; published online 6 June 2016)

Because of its intimate relation with Alzheimer's disease (AD), the question of how amyloid-β peptide (Aβ) deposition alters the membrane and cytoskeltal structure of neural cells and eventually their mechanical response has received great attention. In this study, the viscoelastic properties of primary neurons subjected to various Aβ treatments were systematically characterized using atomic force microrheology. It was found that both the storage (G') and loss (G'') moduli of neural cells are rate-dependent and grow by orders of magnitude as the driving frequency ω varies from 1 to 100 Hz. However, a much stronger frequency dependence was observed in the loss moduli (with a scaling exponent of $\sim$0.96) than that in G' ($\sim\omega^{0.2}$). Furthermore, both cell moduli increase gradually within the first 6 h of Aβ treatment before steady-state values are reached, with a higher dosage of Aβ leading to larger changes in cell properties. Interestingly, we showed that the measured neuron response can be well-explained by a power law structural damping model. Findings here establish a quantitative link between Aβ accumulation and the physical characteristics of neural cells and hence could provide new insights into how disorders like AD affect the progression of different neurological processes from a mechanics point of view. *Published by AIP Publishing.*
[http://dx.doi.org/10.1063/1.4952704]

I. INTRODUCTION

Alzheimer's disease (AD) as one of the most common and devastating neurodegenerative disorders has been attracting researchers from various disciplines in the past few decades. Several lines of evidence suggest that the deposition of amyloid-β (Aβ) peptide is heavily involved in the pathogenesis of AD.[1–3] For example, Aβ was found to be the main constituent of amyloid plaques in the brain of AD patients.[4,5] In addition, it has been shown that endogenous factors that increase the rate of amyloid formation could accelerate the onset of AD, whereas those that inhibit Aβ formation may slow its progression.[6] For this reason, intense efforts have been devoted to examine the toxical effects of Aβ on neural cells. In particular, it was reported that binding of Aβ to the cell membrane results in a marked increase in membrane permeability,[7] along with a reduced fluditity[8,9] and dysregulation of calcium homeostasis.[10–12]

Interestingly, via the single-cell compression test, a recent study indicated that the rigidity of neurons will increase significantly after Aβ treatment.[13] However, since the measurement was conducted on the whole cell level there, the resistance exhibited by the cell is likely mainly due to the cytoplasmic fluid, rather than the membrane-cytoskeleton. Indeed, the apparent moduli of neural cells were reported to be of the order of $\sim$1 MPa in that study which is much higher than those estimated from local testing methods like nano-indentation,[14,15] magnetic, or optical trap stretching.[16] In addition, it also appears to us that how the viscous response of neurons is influenced by Aβ deposition has not been carefully examined. Given that different neurological processes can take place over a wide spectrum of time-scales, this problem could be critical in our understanding of how AD pathogenesis affects the ability of neural cells in executing their biological duties.

Here, by using atomic force microscopy (AFM),[17,18] we systematically characterized the viscoelastic response of primary neurons from the micro-rheology test[19–22] or, more specifically, dynamical mechanical indentation.[23,24] In particular, the complex shear modulus of cells, undergoing various Aβ treatments, was precisely measured over the frequency range of 1–100 Hz. It was found that the appearance of Aβ will lead to a gradual increase in both the storage and loss moduli of cells in the first 6 h before both quantities become saturated. Furthermore, a higher dosage of Aβ resulted in larger changes in cell properties. Lastly, we showed that the measured rheological response of neurons can be well-explained by a power law structural damping model.

II. THEORY OF AFM MICRO-RHEOLOGY

According to the Hertz theory, when a rigid sphere with radius R is pushed into the cell (treated as an elastic half-space) with an indentation depth of δ, the total contact force can be expressed as[22]

[a)]Z. Gong and R. You contributed equally to this work.
[b)]Author to whom correspondence should be addressed. Electronic mail: ylin@hku.hk

$$F = \frac{8}{3}\frac{G}{1-\upsilon}R^{1/2}\delta^{3/2}, \tag{1}$$

where G and υ are the so-called shear moduli and Poisson's ratio of the cell. Taylor expansion of Eq. (1) around a fixed indentation depth δ_0 leads to

$$F = F_0 + \frac{8}{3}\frac{G}{1-\upsilon}R^{\frac{1}{2}}\left[\frac{3}{2}{\delta_0}^{1/2}\Delta\delta + \mathrm{O}(\Delta\delta^2)\right]. \tag{2}$$

Here, $F_0 = \frac{8}{3}\frac{G}{1-\upsilon}R^{1/2}{\delta_0}^{3/2}$ and $\Delta\delta$ can be interpreted as driving oscillations (of the indenter) introduced during the micro-rheology test, refer to Fig. 1. Neglecting higher order terms, Eq. (2) reduces to

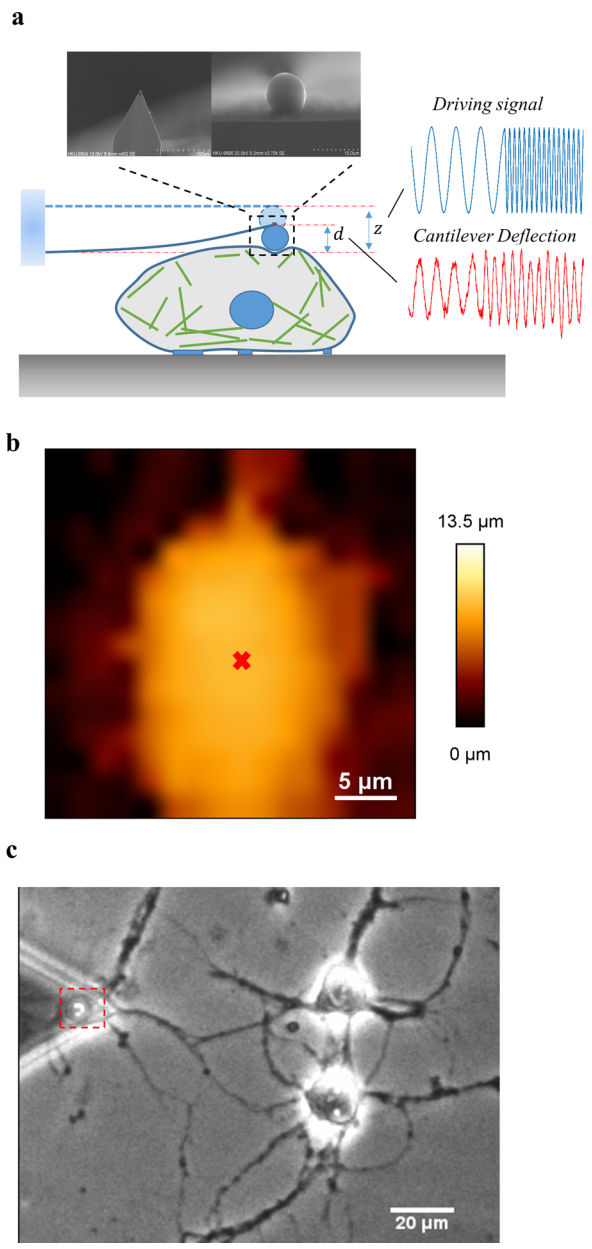

FIG. 1. (a) Schematic plot of the micro-rheology test. Images of the AFM probe used are given in the insets. (b) Height scanning image of the main body of a neural cell. The cross marker indicates the location where the indentation test was conducted. (c) Representative image of neural cells in our experiment. The triangle on the left is the AFM cantilever, while the circle in the red rectangle is the spherical indenter.

$$G = \frac{1-\upsilon}{4(R\delta_0)^{1/2}}\frac{\Delta F}{\Delta\delta}, \tag{3}$$

where $\Delta F = F - F_0$ is the oscillation in the contact force that can be monitored from the deflection of the AFM cantilever (i.e., readout of the test). Converting Eq. (3) into the frequency domain, we have

$$G^*(\omega) = \frac{1-\upsilon}{4(R\delta_0)^{1/2}}\frac{F(\omega)}{\delta(\omega)}, \tag{4}$$

in which $F(\omega)$ and $\delta(\omega)$ represent the Fourier transforms of F and δ, respectively, and $G^*(\omega)$ is the so-called complex shear modulus in this case. Because the experiment was conducted in liquid, a correction term $-i\omega b(0)$ must be added here to take into account the influence of hydrodynamic drag,[25] leading to a final expression of $G^*(\omega)$ as

$$G^*(\omega) = \frac{1-\upsilon}{4(R\delta_0)^{\frac{1}{2}}}\left[\frac{F(\omega)}{\delta(\omega)} - i\omega b(0)\right] \tag{5}$$

(see supplementary material[26] for more details). The complex shear modulus can be decomposed into the real (called the storage moduli G') and imaginary (often referred to as the loss moduli G'') parts, i.e., $G^*(\omega) = G'(\omega) + iG''(\omega)$, which characterize the elastic and viscous resistance of the material against the imposed cyclic deformation. For simplicity, the Poisson's ratio υ is taken to be 0.5 throughout this study, i.e., the cell is assumed to be incompressible.

III. MATERIALS AND METHODS

A. Cell preparation

Cortical neuron cells, obtained from dissecting the brain of 17-day-old Sprague-Dawley rats, were seeded on glass bottom dishes coated with poly-L-lysine (PLL) and maintained at 37 °C in a humidified atmosphere with 5% CO_2 supply. When preparing the dishes, 5 mg of PLL powder was dissolved in sterile Phosphate-buffered saline. 2 ml of the PLL solution was then added on a glass bottom dish and placed in a 37 °C incubator overnight. After that, the PLL solution was removed and the dish was rinsed with autoclaved milli-Q water once. 24 h after the cells were seeded on the PLL-coated dish, 5′-deoxy-5-fluorouridine (5′-DFUR) was added to remove the proliferating cells, including glial and fibroblast cells, while neurons will not be affected and stay attached.

In the meantime, Aβ42 oligomers were dissolved in autoclaved milli-Q water and incubated at 37 °C environment for 24 h. After that, healthy neurons were kept in serum free Supplemented Minimum Essential Media medium containing 1 μM Aβ42 oligomers with different durations (i.e., 1, 3, 6, 12, and 24 h). All tests were conducted at 25 °C after Aβ42 solution was replaced with Dulbecco's Modified Eagle's Medium (DMEM).

B. AFM scanning and indentation test

Micron-sized polystyrene beads (9.75 μm in diameter as shown in the inset of Fig. 1(a)) were glued to flexible tip-less

cantilevers (Arrow TL1-50, Nano-World). After 24 h of waiting for glue stabilization, the optical sensitivity and spring constant of the bead-glued cantilever, assembled into the AFM (NanoWizard® II, JPK Instruments), was calibrated by indenting on glass. The same cantilever was then excited at different frequencies (and oscillation amplitudes) in pure water to calibrate the hydrodynamic drag and piezo lag (see supplementary material[26] for details).

During the test, a fast AFM scanning was first conducted over the live neuron to obtain its morphology (Fig. 1(b)). The center of the cell body (represented by the cross marker in Fig. 1(b)) was then indented by the bead-glued cantilever until a contact force of 0.5nN was reached. After that, oscillations of the cantilever holding base (with 35 nm in amplitude) were introduced at different frequencies. Both the cantilever deflection d and its base height z were recorded at a sampling rate of 2048 Hz and processed by Fast Fourier Transform (FFT). From simple geometry, the actual indentation depth can be estimated as $\delta = z - d$ (Fig. 1(a)). Note that a moderate contact force of 0.5 nN was selected here to make sure that no (or very little) cell damage will be induced. In addition, 12 different cells were tested in each group (i.e., with different durations and dosages of Aβ treatment).

IV. RESULTS AND DISCUSSIONS

A representative force curve from our micro-rheology test is given in Fig. 2(a). Basically, different oscillation frequencies were applied to the AFM holding base leading to distinct temporal response of the contact force. Because of the viscoelastic nature of the cytoskeleton, a phase lag between the driving signal (blue line in the inset of Fig. 2(a)) and the force response (red line) can be detected, allowing us to calculate both the storage and loss moduli of neural cells as shown in Fig. 2(b). The measured storage (or loss) moduli of neurons is in the range of ~50–100 Pa (or ~10–500 Pa) as the driving frequency varies from 1 to 100 Hz, in broad agreement with tests conducted on other cell types. One feature that can immediately be seen is that both moduli increase monotonically with the driving frequency ω. However, a much stronger dependence on the excitation frequency was observed in the loss moduli, with G'' approximately scaling with ω as $G'' \sim \omega^{0.96}$ (in contrast to an exponent around 0.2 for G') when ω is larger than ~10 Hz. Given that G' and G'' describe how fast the stress increases with the strain and the strain rate in the rheology test, respectively, these two quantities essentially characterize the elastic and viscous response of the material. In this regard, our results suggest that the behavior of neural cells at low frequencies is solid-like while the viscous effect becomes dominant in the high frequency regime, in agreement with previous findings on other cell types.[19,27] Such transition is best reflected by the ratio between G'' and G', often referred to as the loss tangent, whose value increases almost 10 times (from 0.3 to 3, refer to Fig. 2(c)) as ω varies from 1 to 100 Hz. Physically, it is conceivable that a slowly imposed strain will be largely absorbed by the elastic deformation of the cytoskeleton. In comparison, most energy will be dissipated through the flow of the viscous cytoplasm, as well as its relative sliding with the cell cortex, at high frequencies.

The complex moduli of neurons, after different durations of Aβ treatment, as functions of ω are shown in Fig. 3(a). Evidently, a longer exposure time to Aβ will lead to higher

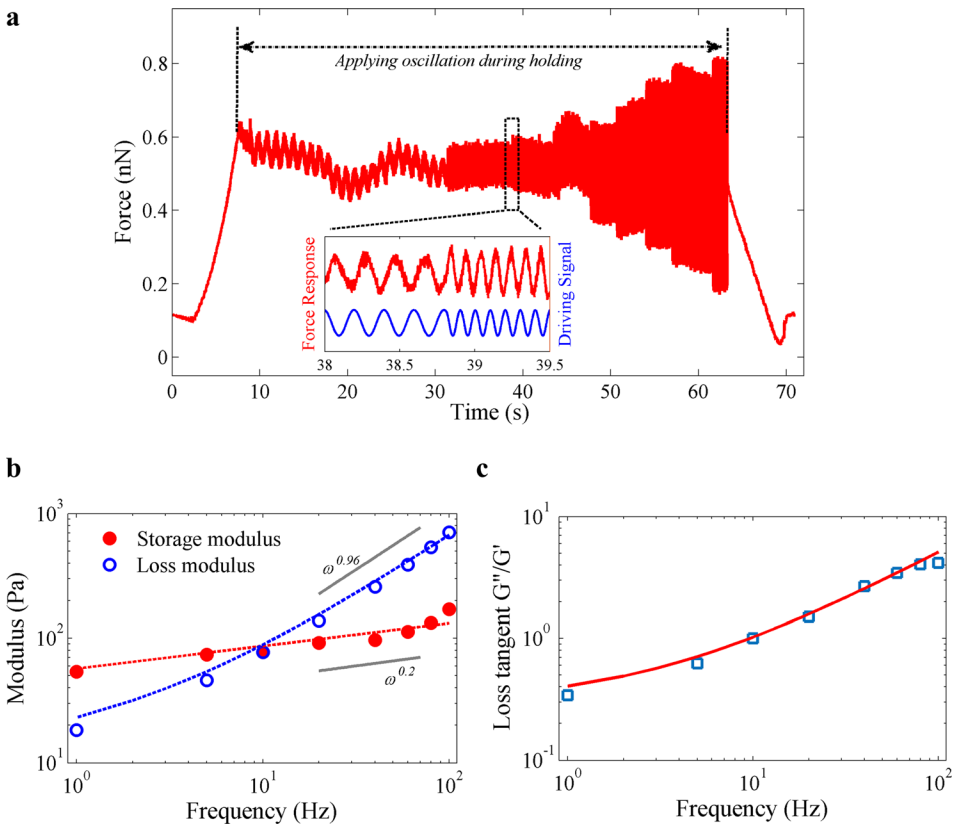

FIG. 2. (a) Typical temporal response of the contact force during micro-rheology test of neurons. The amplified force response (red line), along with the driving signal (blue line), is shown in the inset. (b) Representative storage and loss moduli of neural cells, as functions of the driving frequency, obtained in our experiment. Predictions from the structural damping model (i.e., Eq. (6)) are shown by the dash lines. The two grey lines indicate different power law dependence of cell moduli on the oscillation frequency. (c) Dependence of the loss tangent (i.e., G''/G') of neurons on the driving frequency. Measurement data are represented by symbols while fitting from Eq. (6) is shown by the solid line.

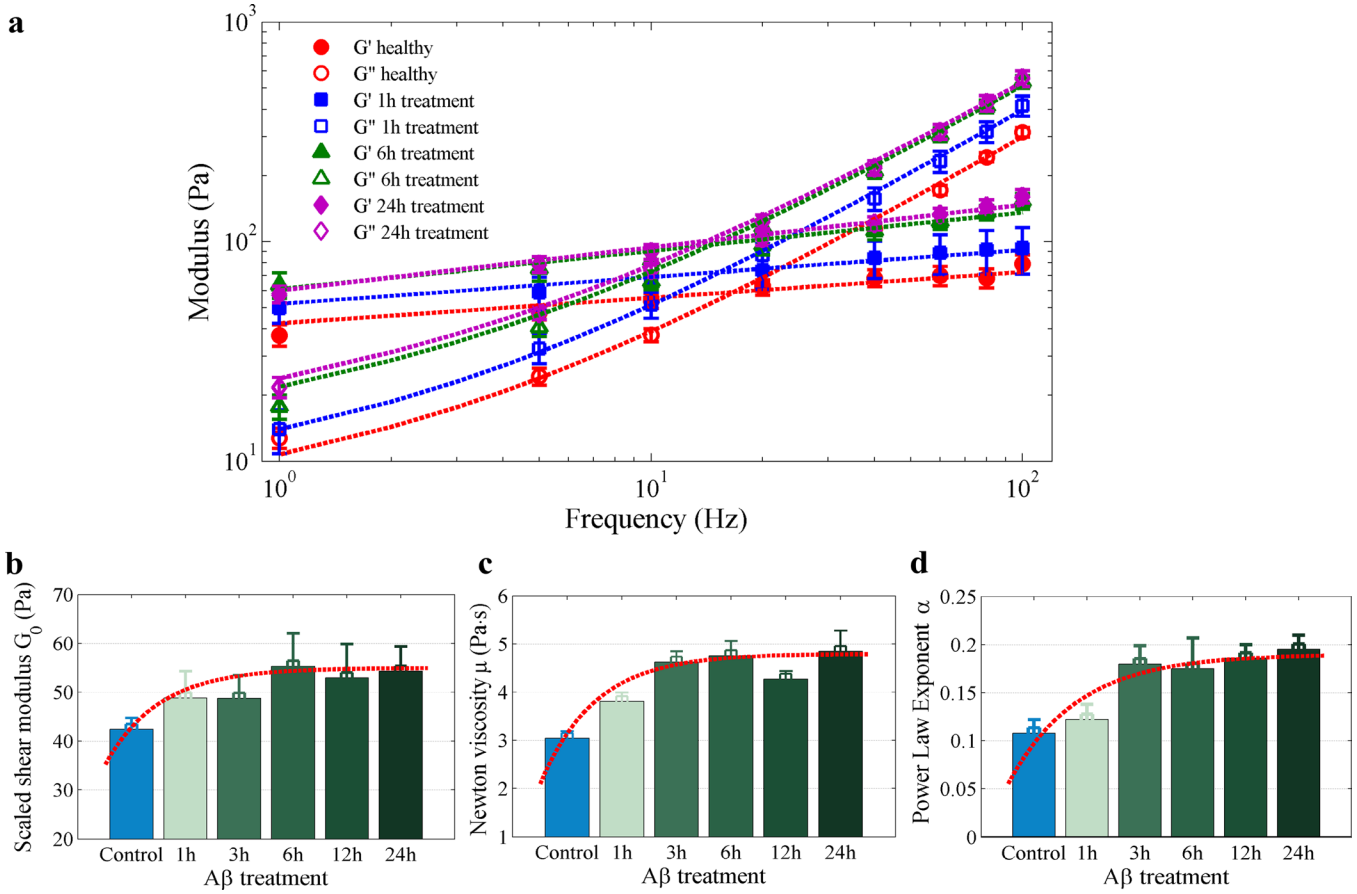

FIG. 3. (a) Frequency-dependent moduli of neural cells after different durations of Aβ (1 μM) treatment. (b) and (c) The scaled shear modulus (b), newton viscosity (c), and power law exponent (d) of neurons extracted by fitting experimental data with the structural damping model, i.e., Eq. (6). Results shown here are based on measurements on 12 cells in each group. Error bar represents the standard error of the mean (SEM).

values in both G' and G'', and hence the apparent elastic shear modulus and viscosity of cells. However, such increase becomes saturated after ~6 h (Figs. 3(b) and 3(c)). Besides duration, we also examined the influence of Aβ concentration on neuron properties. As shown in Fig. 4, a positive correlation between the Aβ dosage and cell moduli has been observed. The Student's t test confirmed that both the storage and loss moduli of cells treated with different dosages of Aβ for 6 h are significantly higher than the control group ($p < 0.05$) at all frequencies. Interestingly, most neurons tested (control or after Aβ treatment) exhibit similar scaling relationships as those shown in Fig. 2(b). Specifically, histograms of the two scaling exponents describing the dependence of G' or G'' on ω from our measurements are given in Fig. 5, which again indicates that the loss modulus increases much faster with ω compared to G'.

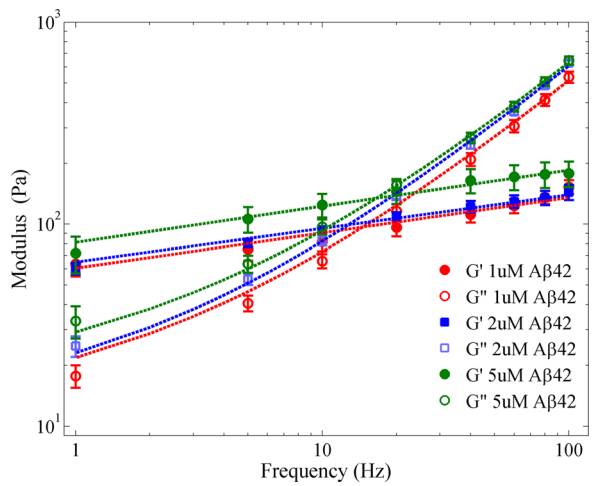

FIG. 4. Storage and loss moduli of neural cells after different dosages of Aβ treatment (for 6 h). 12 cells were tested in each group where the standard error of the mean (SEM) is shown by the error bar.

It must be pointed out that studies have shown that Aβ peptides can self-aggregate into fibrils that have a stable anti-parallel β-sheet structure[28] and a stiffness of the order of GPa.[29] As such, it is natural to believe that the addition/insertion of such fibrils in the membrane or the cytoskeleton[30] (Fig. 6(a)) will increase the apparent rigidity of cells. On the other hand, transient binding and entanglement between Aβ fibril and lipid molecule or F-actin can also significantly lower the fluidity of the membrane-cortex layer,[31] manifesting as the elevated moduli of Aβ-treated neurons observed here. This line of reasoning is further corroborated by recent observations that the aggregation of Aβ will take several hours to complete *in vitro*.[32,33] In addition, it has also been shown that the intensity of fluorescently tagged Aβ(1–42) in live cells will reach the maximum in ~5–8 h (and stay at that level afterward),[34] in good agreement with

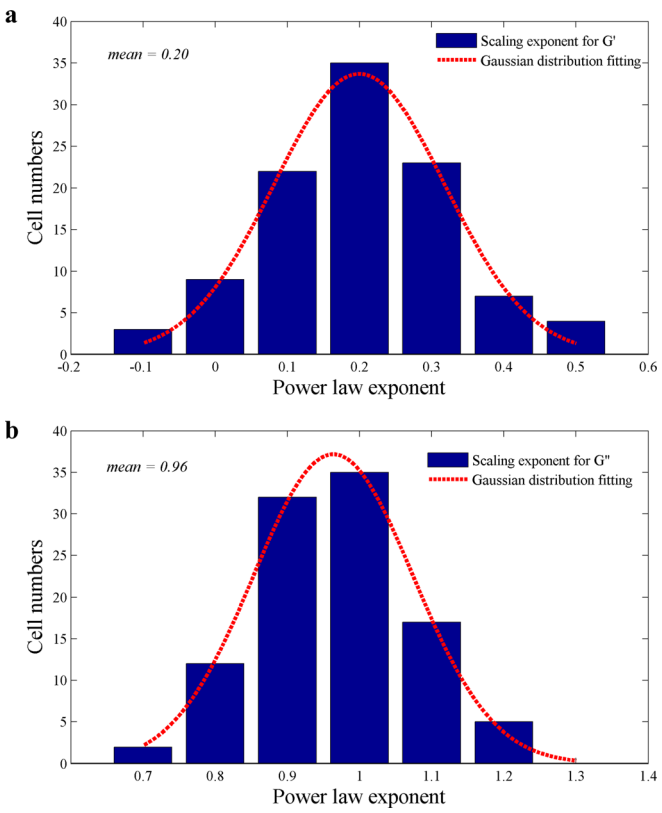

FIG. 5. Histogram of the scaling exponent between G' (a) or G'' (b) and the driving frequency. The red dash lines show the distributions are more or less Gaussian. Results here are based on tests conducted on 103 control and Aβ-treated cells.

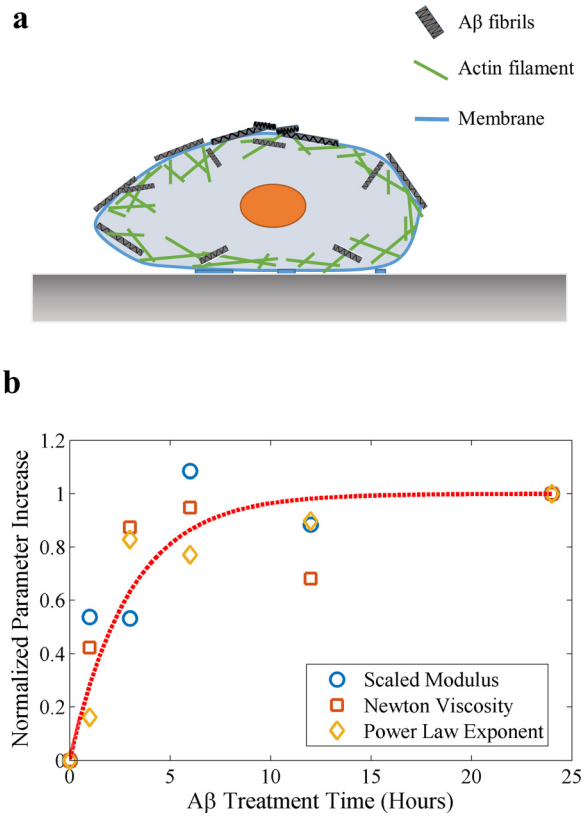

FIG. 6. (a) Schematic plot showing the formation/insertion of Aβ fibrils in the membrane-cortex layer, eventually leading to elevated apparent rigidity and viscosity of cells. (b) Normalized increases in the three fitting parameters (in the power law structural damping model) with respect to Aβ (1 μM) treatment time.

our finding that the increase in cell moduli becomes saturated after around 6 hours of Aβ treatment.

Finally, to gain more physical insights on the frequency dependency, we proceeded by seeking phenomenological models that can explain these observations. It soon became clear to us that neither simple spring-dashpot based models nor conventional power law relations[35,36] can fit our data well. However, the so-called power law structural damping model[19,37] seems to work where G^*, in this case, was assumed to depend on the driving frequency as

$$G^*(\omega) = G_0(1 + i\eta)\left(\frac{\omega}{\omega_0}\right)^{\alpha} + i\omega\mu. \tag{6}$$

Here, G_0 and μ represent the scaled shear modulus and newton viscosity of the material, respectively, α is the power law parameter, and $\eta = \tan(\alpha)$ is referred to as the structural damping coefficient. ω_0 is a normalization frequency often taken to be 1 Hz.[19] Interestingly, it appears that both the storage and shear moduli obtained from our tests can be explained by Eq. (6). Specifically, choosing fitting parameters (i.e., G_0, μ, and α) as listed in Tables I and II, predictions from Eq. (6) are given by the dashed lines in Figs. 2(b), 2(c), 3(a), and 4 which clearly fit measurement data very well. In addition, not surprisingly, these three parameters all increase gradually within the first 6 h of Aβ treatment before reaching their steady-state values (Figs. 3(b)–3(d) and 6(b)).

V. CONCLUSION

In this study, we systematically examined (for the first time we believe) how the dynamic behavior of neural cells is affected by Aβ treatment via a micro-rheology test. In contrast to previous investigations where a static compression was applied to the entire cell,[13] the present approach allows us to extract the viscous response of neurons over a wide range of excitation frequencies. In addition, because of the local probing nature of AFM indentation, our results should also reflect the membrane/cytoskeletal changes induced by Aβ deposition

TABLE I. Parameter values used in the structural damping model to fit experimental data on neurons after different durations of Aβ treatment.

Parameters	In control	1 h Aβ treatment	3 h Aβ treatment	6 h Aβ treatment	12 h Aβ treatment	24 h Aβ treatment
α	0.108 ± 0.014	0.122 ± 0.016	0.180 ± 0.019	0.175 ± 0.032	0.186 ± 0.014	0.195 ± 0.015
G_0 (Pa)	42.37 ± 2.38	48.81 ± 5.53	48.74 ± 4.78	55.36 ± 6.70	52.95 ± 6.93	54.34 ± 5.03
μ (Pa s)	3.043 ± 0.143	3.809 ± 0.186	4.624 ± 0.228	4.757 ± 0.311	4.275 ± 0.167	4.852 ± 0.425

TABLE II. Parameter values used in the structural damping model to fit experimental data on neurons treated with different dosages of Aβ.

Aβ concentration (μM)	Exponent α	Scaled modulus G_0 (Pa)	Newton viscosity μ (Pa s)
1.0	0.175 ± 0.032	55.36 ± 6.70	4.757 ± 0.311
2.0	0.166 ± 0.018	59.59 ± 2.94	5.690 ± 0.173
5.0	0.179 ± 0.020	74.08 ± 8.51	5.771 ± 0.291

(or the progression of AD), something that may not be achievable by tests conducted on the whole-cell level.

Our experiments suggested that both rigidity and viscosity of neurons increase due to the presence of Aβ. Furthermore, a longer exposure time to (or a higher dosage of) Aβ will lead to larger values in the apparent shear modulus and newton viscosity of cells although such increase becomes saturated after ~6 h of treatment. It is conceivable that the elevated elastic modulus is caused by the addition/insertion of rigid Aβ fibrils on the membrane or in the cytoskeleton.[30] At the same time, transient interactions between Aβ fibril and lipid molecule or F-actin can reduce the fluidity of the membrane-cortex layer[31] and result in an increase in the apparent viscosity of cells. Given that different neurological processes can take place over a wide spectrum of timescales, findings here could greatly help us understand the possible correlation between AD pathogenesis and the ability of neural cells in executing their biological duties. For example, the elevated rigidity and viscosity could stall neurite outgrowth,[38] reduce neuronal motility,[39] and hence impair signal transmission among neural cells.

The measured storage (or loss) modulus of neurons is in the range of ~50–100 Pa (or ~10–500 Pa) as the driving frequency varies from 1 to 100 Hz, in broad agreement with tests conducted on other cell types. It seems that all our data can be well-explained by the power law structural damping model,[19,37] with the fitting power law coefficient of the order of 0.1–0.2 which is comparable to that suggested by other studies.[19,20,36,40,41] Nevertheless, the interesting finding that G' and G'' scale with ω with the exponent ~0.2 and ~0.96, respectively, is different from the 3/4 power law dependence reported for other biopolymer materials.[42–44] From a modeling point of view, it is possible to combine existing formulations of Aβ aggregation, such as the nucleated polymerization[32] and kinetic fibrillogenesis theories,[45] with proper constitutive descriptions regarding how stiff Aβ fibril interacts with other constituents in the membrane-cortex layer to predict the rheological response of neural cells undergoing Aβ treatment. However, this is beyond the scope of the present study. In addition, we have limited our attention to the frequency range of 1–100 Hz here because the force response will be overwhelmed by noise (i.e., thermal fluctuations) at very low frequencies. On the other hand, the nonlinear nature of hydrodynamic forces, as well as possible resonance effect of the AFM cantilever, also make the accurate measurement at high frequencies extremely difficult in our setup. Further investigations are certainly warranted to address these issues.

ACKNOWLEDGMENTS

This work was supported by grants from the Research Grants Council (Project Nos. HKU 714312E, HKU 714713 E, and HKU 17205114) of the Hong Kong Special Administration Region and the National Natural Science Foundation of China (Project No. 11572273).

[1]J. Hardy and D. J. Selkoe, Science **297**, 353 (2002).
[2]A. E. Roher, M. O. Chaney, Y. M. Kuo, S. D. Webster, W. B. Stine, L. J. Haverkamp, A. S. Woods, R. J. Cotter, J. M. Tuohy, G. A. Krafft, B. S. Bonnell, and M. R. Emmerling, J. Biol. Chem. **271**, 20631 (1996).
[3]I. Costantino, Nat. Rev. Neurosci. **5**, 347 (2004).
[4]G. Glenner and C. W. Wong, Biochem. Biophys. Res. Commun. **120**, 885 (1984).
[5]G. Shankar, S. M. Li, T. Mehta, A. Garcia-Munoz, N. Shepardson, I. Smith, F. Brett, M. A. Farrell, M. Rowan, C. Lemere, C. M. Regan, D. M. Walsh, B. Sabatini, and D. Selkoe, Nat. Med. **14**, 837 (2008).
[6]D. J. Selkoe and D. Schenk, Annu. Rev. Pharmacol. Toxicol. **43**, 545 (2003).
[7]R. Kayed, Y. Sokolov, B. Edmonds, T. M. McIntire, S. C. Milton, J. E. Hall, and C. G. Glabe, J. Biol. Chem. **279**, 46363 (2004).
[8]J. J. Kremer, M. M. Pallitto, D. J. Sklansky, and R. M. Murphy, Biochemistry **39**, 10309 (2000).
[9]W. E. Müller, G. P. Eckert, K. Scheuer, N. J. Maras, A. Gattaz, W. F. Müller, W. F. Eckert, W. F. Cairns, and W. F. Gattaz, Amyloid **5**, 10 (1998).
[10]R. Brackenbury, U. Rutishauser, and G. M. Edelman, Proc. Natl. Acad. Sci. U. S. A. **78**, 387 (1981).
[11]K. N. Green and F. M. LaFerla, Neuron **59**, 190 (2008).
[12]A. Demuro, I. Parker, and G. Stutzmann, J. Biol. Chem. **285**, 12463 (2010).
[13]V. Lulevich, C. C. Zimmer, H.-S. Hong, L.-W. Jin, and G.-Y. Liu, Proc. Natl. Acad. Sci. U. S. A. **107**, 13872 (2010).
[14]B. Tang and A. Ngan, Soft Matter **8**, 5974 (2012).
[15]Z. L. Zhou, A. H. W. Ngan, B. Tang, and A. X. Wang, J. Mech. Behav. Biomed. **8**, 134 (2012).
[16]T. Hui, Q. Zhu, Z. Zhou, J. Qian, and Y. Lin, Appl. Phys. Lett. **105**, 073703 (2014).
[17]E. G. Herbert, W. C. Oliver, and G. M. Pharr, J. Phys. D: Appl. Phys. **41**, 074021 (2008).
[18]Y. Cao, X. Ji, and X. Feng, Sci. China: Phys., Mech. Astron. **54**, 598 (2011).
[19]J. Alcaraz, L. Buscemi, M. Grabulosa, X. Trepat, B. Fabry, R. Farre, and D. Navajas, Biophys. J. **84**, 2071 (2003).
[20]P. Cai, Y. Mizutani, M. Tsuchiya, J. Maloney, B. Fabry, K. Van Vliet, and T. Okajima, Biophys. J. **105**, 1093 (2013).
[21]R. E. Mahaffy, C. K. Shih, F. C. Mackintosh, and J. Käs, Phys. Rev. Lett. **85**, 880 (2000).
[22]R. E. Mahaffy, S. Park, E. Gerde, J. Käs, and C. K. Shih, Biophys. J. **86**, 1777 (2004).
[23]C. A. Grant, P. C. Twigg, and D. J. Tobin, Acta Biomater. **8**, 4132 (2012).
[24]C. A. Grant, M. A. Phillips, and N. H. Thomson, J. Mech. Behav. Biomed. **5**, 165 (2012).
[25]J. Alcaraz, L. Buscemi, M. Puig-de-Morales, J. Colchero, A. Baro, and D. Navajas, Langmuir **18**, 716 (2002).
[26]See supplementary material at http://dx.doi.org/10.1063/1.4952704 for the calibration deatials of the micro-rheology test.
[27]J. Rother, H. Nöding, I. Mey, and A. Janshoff, Open Biol. J. **4**, 140046 (2014).
[28]R. M. Murphy, Annu. Rev. Biomed. Eng. **4**, 155 (2002).
[29]A. Fitzpatrick, S. Park, and A. Zewail, Proc. Natl. Acad. Sci. U. S. A. **110**, 10976 (2013).
[30]I. W. Hamley, Chem. Rev. **112**, 5147 (2012).
[31]Y. Verdier, M. Zarándi, and B. Penke, J. Pept. Sci. **10**, 229 (2004).
[32]P. Hortschansky, V. Schroeckh, T. Christopeit, G. Zandomeneghi, and M. Fändrich, Protein Sci. **14**, 1753 (2005).
[33]E. Hellstrand, S. Linse, B. Boland, and D. M. Walsh, ACS Chem. Neurosci. **1**, 13 (2010).
[34]E. K. Esbjörner, F. Chan, E. Rees, M. Erdelyi, L. M. Luheshi, C. W. Bertoncini, C. F. Kaminski, C. M. Dobson, and G. S. Kaminski Schierle, Chem. Biol. **21**, 732 (2014).
[35]M. M. Brandao, A. Fontes, M. L. Barjas-Castro, L. C. Barbosa, F. F. Costa, C. L. Cesar, and S. T. O. Saad, Eur. J. Haematol. **70**, 207 (2003).

[36]M. Balland, N. Desprat, D. Icard, S. Fereol, A. Asnacios, J. Browaeys, S. Henon, and F. Gallet, Phys. Rev. E **74**, 021911 (2006).
[37]B. Fabry, G. N. Maksym, J. P. Butler, M. Glogauer, D. Navajas, and J. J. Fredberg, Phys. Rev. Lett. **87**, 148102 (2001).
[38]A. Mogilner and B. Rubinstein, Biophys. J. **89**, 782 (2005).
[39]C. Xie, L. Hanson, W. Xie, Z. Lin, B. Cui, and Y. Cui, Nano Lett. **10**, 4020 (2010).
[40]J. Maloney, E. Lehnhardt, A. Long, and K. Van Vliet, Biophys. J. **105**, 1767 (2013).
[41]E. Zhou, S. Quek, and C. Lim, Biomech. Model. Mechanobiol. **9**, 563 (2010).
[42]F. Gittes, B. Schnurr, P. D. Olmsted, F. Mackintosh, and C. Schmidt, Phys. Rev. Lett. **79**, 3286 (1997).
[43]F. Gittes and F. C. MacKintosh, Phys. Rev. E **58**, R1241 (1998).
[44]M. L. Gardel, J. H. Shin, F. C. Mackintosh, L. Mahadevan, P. A. Matsudaira, and D. A. Weitz, Phys. Rev. Lett. **93**, 188102 (2004).
[45]A. Lomakin, D. Teplow, D. Kirschner, and G. B. Benedek, Proc. Natl. Acad. Sci. U. S. A. **94**, 7942 (1997).